IOPscience iopscience.iop.org

Home Search Collections Journals About Contact us My IOPscience

First-principles study of the lattice dynamics of c(2 × 2)-CO on Cu(001)

This article has been downloaded from IOPscience. Please scroll down to see the full text article.

2008 J. Phys.: Condens. Matter 20 224009

(http://iopscience.iop.org/0953-8984/20/22/224009)

View the table of contents for this issue, or go to the journal homepage for more

Download details:
IP Address: 129.252.86.83
The article was downloaded on 29/05/2010 at 12:29

Please note that terms and conditions apply.

J. Phys.: Condens. Matter **20** (2008) 224009 (7pp) doi:10.1088/0953-8984/20/22/224009

First-principles study of the lattice dynamics of c(2 × 2)-CO on Cu(001)

Marisol Alcántara Ortigoza[1,2], Talat S Rahman[1], Rolf Heid[2] and Klaus-Peter Bohnen[2]

[1] Department of Physics, University of Central Florida, Orlando, FL 32816, USA
[2] Forschungszentrum Karlsruhe, Institut für Festkörperphysik, D-76021 Karlsruhe, Germany

E-mail: alcantar@physics.ucf.edu, talat@physics.ucf.edu, heid@ifp.fzk.de and bohnen@ifp.fzk.de

Received 8 November 2007, in final form 21 January 2008
Published 13 May 2008
Online at stacks.iop.org/JPhysCM/20/224009

Abstract
The density-functional perturbation theory formalism is applied to investigate the dynamics of c(2 × 2)-CO/Cu(100), using both the local (LDA) and the generalized-gradient (GGA) density approximations through the Hedin–Lundqvist and the Perdew–Burke–Ernzerhof functionals, respectively. In the framework of the mixed basis pseudopotential approach, GGA reproduces notably well helium atom scattering (HAS) data for the frustrated translation (FT) mode and hence points to a harmonic nature of the Cu–C bond. LDA, on the other hand, is found to lead to instabilities of the FT mode inside the surface Brillouin zone (SBZ). The C–O internal stretch mode disperses in the two-dimensional SBZ by ∼10 meV along the Δ direction. The Cu–CO stretch mode involves a significant contribution from first-layer Cu atoms. The frustrated rotation and FT modes disperse slightly and have their degeneracy removed by ∼1 meV and ∼3 meV, respectively, along the Σ direction. The latter is in quantitative agreement with HAS data.

1. Introduction

Comprehension of the coupling between molecules and metallic surfaces have attracted much interest in the last three decades [1, 2] because of the insight it provides into chemisorption and diffusion processes [3], which ultimately control phenomena such as catalysis and corrosion. In this regard, *ab initio* numerical methods based on the density-functional theory (DFT) represent, to date, the most robust and accurate approach to model, understand, and predict the geometrical, electronic, and dynamical properties of chemisorbed surfaces, as well as many other systems. Of particular relevance in this work is the density-functional perturbation theory (DFPT), which furnishes a powerful and comprehensive framework to deal with perturbations in the ionic positions since it provides access to the dynamics of the adsorbate and the substrate in the entire surface Brillouin zone (SBZ) while taking into consideration all interatomic couplings within the system [4]. On the experimental side, different spectroscopic techniques, such as infrared-reflection absorption spectroscopy (IRRAS) and Raman and electron energy loss spectroscopy (EELS), have provided a vast amount of data on vibrational modes whose frequencies exceed ∼20 meV [5]. Inelastic helium atom scattering (HAS) has instead been the leading technique for measuring frequencies below ∼20 meV, particularly those arising from fluctuations of the surface–molecule bond, as manifested in the frustrated translation (FT) modes of adsorbed molecules [6].

The CO/Cu(100) system has been widely studied because of its structural symmetry, relatively simple electronic structure, and experimental approachability [7]. Low energy electron diffraction (LEED) and near-edge x-ray adsorption fine structure (NEXAFS) measurements show that CO adsorbs on Cu(001) with the C end bound atop Cu surface atoms and the molecular bond oriented normal to the surface, forming a c(2 × 2) overlayer at half monolayer, $\theta = 0.5$ ML (see figure 1(a)) [2, 8–10]. Vibrational modes of CO on Cu(001) have also been extensively studied experimentally [11] and theoretically at the center of the SBZ [1, 12], the Γ-point (see figure 1(b)). Their dispersion has been assessed experimentally only in the low frequency range by HAS [6]. To our knowledge, no attempt to obtain theoretically the phonon dispersion relations of the chemisorbed surface has so far been carried out.

 © 2008 IOP Publishing Ltd Printed in the UK

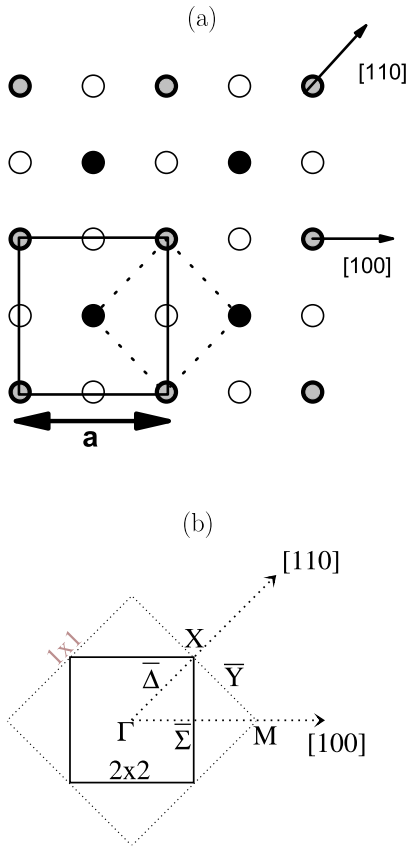

Figure 1. (a) The top view of the surface shows CO (gray dots), and first (filled circles) and second (open circles) layer atoms of Cu(100). The 1×1 (dashed line) and the c(2×2) (solid line) surface unit cells are underlined. (b) The corresponding (1×1) (dotted line) and c(2×2) surface Brillouin zones (solid line) showing the Γ, X, and M points; and the Δ, Σ, and Y directions.

The vibrational modes of CO on the Cu(001) surface may be divided into two groups according to their polarization. The first group involving displacements perpendicular to the surface are the C–O and the Cu–CO stretch modes, whose frequencies are denoted by ν_1 and ν_2, respectively. The second group involves mostly horizontal displacements derived from the rotational and translational motions of the free CO molecule that become frustrated upon adsorption on the Cu surface [6]. The four modes among this group consist of two frustrated rotation (FR) modes and two frustrated translation (FT) modes, whose frequencies are denoted by ν_3 and ν_4, respectively. Notice that straight atop adsorption of the molecule on the (001) surfaces of fcc metals causes degeneracy in the two FR and FT modes at Γ [6].

Lewis and Rappe [13] computed the frequencies of all six modes at Γ, treating both the adsorbate and the substrate on equal footing within the density-functional theory (DFT), applying the local density approximation (LDA) and the finite-differences (FD) method. They found reasonable agreement with experiment for the Rayleigh wave of the substrate, and for ν_1 and ν_3, but not for ν_2 and ν_4. They also found the molecule–substrate bond to be anharmonic with respect to horizontal displacements and that the introduction of anharmonicity effects in the force constants shifted ν_4 very close to the experimental value [13]. Favot *et al* [12], applying the DFPT approach and the generalized-gradient approximation (GGA) via the Perdew–Burke–Ernzerhof (PBE) exchange–correlation functional, obtained values of ν_1 and ν_2 at the Γ point to be in agreement with the experimental data, but ν_3, ν_4 and the frequencies of the substrate modes were not reported. They compared the capabilities of LDA and GGA-PBE to describe c(2×2)-CO/Cu(100), and found that LDA fails to find the top site as the preferred adsorption site of the molecule, while GGA-PBE reproduces it correctly. Through examination of the dispersion of the phonons of c(2×2)-CO/Cu(100) using DFPT, this work shows that LDA, apart from predicting the wrong adsorption site [1, 12], produces negative frequencies for the FT mode almost everywhere in the sampled regions of the SBZ (except in the vicinity of Γ), suggesting-against the experimental evidence—that the CO-c(2×2) overlayer is unstable under the FT mode distortion. Meanwhile, the dispersion of the FT mode obtained from GGA-PBE reproduces quantitatively well HAS measurements without need to adjust the involved force constants to incorporate anharmonic effects [13].

The dynamical instabilities presented by LDA in CO-chemisorbed Cu(001) are linked to the inability of LDA to describe the CO–Cu interaction and to the consequent wrong prediction of the preferred adsorption site of CO. The later problems are in turn derived from the non-exact cancelation of the Coulomb self-interaction inherent to the unknown expression of the exchange–correlation energy in the Kohn–Sham approach [14]. As a matter of fact, neither LDA nor GGA exchange–correlation functionals in the Kohn–Sham potential exhibit the correct asymptotic C/r decay (where C is a constant) in finite systems [14, 15]. The correlation contribution is actually short-ranged so that exchange effects quickly dominate the C/r decay [15]. Indeed, hybrid functionals combining certain portion of the Hartree–Fock (exact) exchange are able to mend the deficiencies of LDA and GGA functionals regarding the adsorption site of CO on metal surfaces [16]. Theoretical studies of CO adsorption on Cu(111) and Pt(111) have shown that a priori tweaking the Hamiltonian with an extra correlation term (GGA + U) [1, 16] or the usage of hybrid functionals (B3LYP) [17, 18] correctly favor atop CO adsorption, sustaining that the theoretically predicted preference for the hollow site adsorption by LDA and GGA follows from the spurious self-interaction [17]. The binding energy and the preference to adsorb either atop or at the hollow site was in turn found to depend on the hybridization between the d-metal states and the 5σ orbital—the highest occupied CO orbital (HOMO)—and that of the d-metal states and the $2\pi^*$ orbital—the lowest unoccupied CO orbital (LUMO) [1, 16]. Donation from the 5σ orbital to the substrate tends to drive the molecule towards the top, whereas back-donation from the substrate to the $2\pi^*$ orbital favors the adsorption at the hollow site [16]. Kresse *et al* hence concluded that the shortcomings of local and semi-local exchange–correlation functionals overestimate the stability of partially occupied states, allowing d-metal states to hybridize more strongly with the $2\pi^*$ orbital (when CO adsorbs at the hollow site) than with the 5σ orbital (when CO adsorbs atop) [16]. GGA-PBE

and GGA-rPBE (revised GGA-PBE) functionals, though not systematically self-interaction free, introduce an enlargement of the 5σ–$2\pi^*$ gap of CO [16, 19, 20], which tends to reduce the hybridization of these orbitals with the d-states of Cu. Consistently, PBE functionals in general produce lower biding energies of CO on Cu(001) and Cu(111) than LDA functionals, to the extent that the binding energy atop significantly approaches to the experimental value [1, 12]. In fact, since the $2\pi^*$ orbital is particularly shifted to higher energies by PBE functionals [16, 19], the discrepancy between theory and experiment about the preferred adsorption site is removed in the case of Cu(001) merely by using GGA-PBE [12]. For Cu(111), however, the wrong prediction of a higher binding energy at the threefold hollow site remains, even though the differences in binding energy between adsorption atop and at the hollow are lowered to 40 meV [1]. The reason why adsorption at the threefold hollow site is still favored in the case of the Cu(111) may be related to the atom density per layer. Namely, the C–Cu distance is ∼0.1 Å shorter for adsorption at the threefold hollow site than for adsorption at the fourfold hollow site [1], a situation which may determine that, only in the former case, the $2\pi^*$–d hybridization be sufficient as to hinder the atop adsorption preference.

The rest of this work is organized as follows. Section 2 contains the computational details for the present calculations. Section 3 is a summary of results concerning the structure of c(2 × 2)-CO/Cu(100). In section 4, we present our results and discussion of the dynamics of c(2 × 2)-CO/Cu(100). Finally, section 5 contains the concluding remarks of this study.

2. Computational details

Periodic super-cell calculations are performed on the basis of the DFT formalism and the pseudopotential approach [4]. The present results are derived from the mixed basis (MB) technique [21], which reduces significantly the size of the basis set to describe valence states that are strongly localized near atomic sites. Results using both LDA and GGA are obtained. The former is applied through the Hedin–Lundqvist [22] parameterization of the exchange–correlation functional, whereas GGA is introduced via the PBE expression [23].

The radius around Cu sites, at which the d-type local functions are smoothly cut off, r_{cutoff}, is 2.3 au for both LDA and GGA-PBE. The r_{cutoff} of s- and p-type local functions is 1.2 and 1.08 au, respectively, for C and O in both LDA and GGA-PBE. In the present GGA-PBE calculations, d-type basis functions are included in the description of the valence states of C atoms. The maximum kinetic energy, E_{max}, of the plane waves used to describe valence states has been set to 20 Ryd for LDA and increased up to 33 Ryd for GGA-PBE to reach convergence of the CO bond length and the atomic forces in c(2 × 2)-CO/Cu(001). The energy at which the Fourier expansion of the charge density is truncated, G_{max}, has been set to 50 Ryd for both LDA and GGA-PBE.

The CO-chemisorbed Cu(001) surface is simulated with symmetric slabs inside a tetragonal unit cell containing either 9 (for LDA) or 7 (for GGA-PBE) layers of Cu. CO molecules are also symmetrically located on each side of the slab. Periodically repeated slabs are separated by a distance equivalent to 9 and 11 layers, correspondingly. Integrations inside the SBZ are done over discrete mesh of 6 × 6 × 1 k-points. Integrations up to the Fermi surface at an irreducible set of k-points are obtained using the broadening technique for the level occupation [24], where the Gaussian smearing parameter, σ, is set to 0.2 eV.

To find the binding energy of a molecule in the c(2 × 2) overlayer, we have taken into account the direct interaction among the molecules. We have thus calculated the total energy of CO molecules in a free-standing two-dimensional c(2 × 2) array as in the c(2 × 2)-CO/Cu(001) system, using the same super-cell employed in the chemisorbed system, as well as all other parameters. The direct-interaction energy among molecules in the above two dimensional array is thus the difference between the total energy of one molecule in the array and that of an isolated molecule. The latter is modeled using a large super-cell of 19 au × 19 au × 21 au, so as to limit integration over only 1 k-point.

Minimization of the slab total energy as a function of the atomic positions is based upon the reduction of Hellman–Feynman forces [25] below 10^{-3} Ryd au^{-1}, using the Broyden–Fletcher–Goldfarb–Shanno (BFGS) algorithm [26].

The calculation of the lattice dynamical matrices at specific q-points of the SBZ is based on the linear response theory embodied within DFPT [4, 27], as developed by Heid and Bohnen [28]. Here, calculations are performed at the q-points of a 2 × 2 × 1 mesh in the SBZ, applying a convergence criterion of 0.02 meV in the phonon energies. The real-space force constants of the c(2×2)-CO/Cu(001) system are obtained by the standard Fourier transform of the above dynamical matrices [29]. The force constants are then matched with those of bulk Cu to model an asymmetric 800-layer slab, and used to obtain the frequencies at arbitrary q-points. Surface modes have been identified as those whose amplitude weight in the 6 outermost atoms, including C and O, is larger than 20%.

3. Structural properties

The c(2 × 2) structure exhibited by the CO adlayer on Cu(001) is illustrated in figure 1(a). Notice there that the primitive super-cell contains two atoms per layer, and that these are non-equivalent in odd numbered layers since CO sits directly above only one of them. Accordingly, atoms in the first layer are referred either as *covered* or *bare* atoms.

The present work and previous calculations [12, 13] indicate that the first and third layers rumple, but not the second layer atoms. As shown in table 1, there are differences in the interlayer relaxations of the Cu(001) surface upon CO adsorption as predicted by LDA and GGA-PBE. To our knowledge, there is no experimental characterization of the substrate geometry after CO adsorption. As for the bond lengths, for which experimental data is available, table 1 shows that GGA gives better agreement than LDA.

The results of our calculated interaction energy among molecules in the free-standing c(2 × 2) array also point to difficulties in the application of LDA to this system: LDA finds

Table 1. Percentage change of the interlayer spacing of the outermost Cu layers of c(2 × 2)-CO on Cu(100) compared to the bulk situation; bond length of CO, d_{C-O}, when it is adsorbed on Cu(001) (on Cu), isolated (free) CO, and in a free-standing c(2 × 2) mesh (mesh); and bond length of the C–Cu bond, d_{Cu-C}. Label A distinguishes the interlayer Cu spacing referred to atoms that have CO directly above, while B accounts for the those which do not.

	Theory					
	LDA			PBE		Experiment
	This work	Ref [13]	Ref [12]	This work	Ref [12]	Refs [8], [33], and [2]
Δd_{12}	$+0.34^{A}$ -2.17^{B}	$+0.50^{A}$ -1.56^{B}	$+1.4^{A}$ -2.7^{B}	$+1.32^{A}$ -4.41^{B}	$+2.0^{A}$ -4.1^{B}	—
Δd_{23}	-0.17^{A} $+0.64^{B}$	$+0.44^{A}$ $+1.39^{B}$	$+0.1^{A}$ $+1.2^{B}$	$+0.02^{A}$ $+0.71^{B}$	$+0.2^{A}$ $+1.7^{B}$	—
Δd_{34}	-0.15^{A} -0.96^{B}	$+0.72^{A}$ -0.40^{B}	—	-0.44^{A} -1.12^{B}	—	—
d_{C-O} (Å)^{chemisorbed}	1.16	1.14	1.15	1.16	1.16	1.15
d_{C-O} (Å)^{mesh}	1.14	—	—	1.15	—	—
d_{C-O} (Å)^{free}	1.14	1.12	1.36	1.14	1.15	1.13
d_{Cu-C} (Å)	1.83	1.85	1.82	1.88	1.88	1.90 ± 0.01

Table 2. Frequencies (in meV) at Γ of the vibrational modes of c(2 × 2)-CO on Cu(001).

	Theory							Experiment
	LDA				PBE			HAS and IRRAS
	This work[a]	Ref [13][b]	Ref [12][a]	Ref [34][c,d]	This work[a]	Ref [12][a]	Ref [34][c,d]	Refs [6] and [5]
ν_1	265.6	261.7	259.8	268.8	257.7	251.2	262.6	258.5
ν_2	54.6	52.9	54.2	49.6	47.4	47.2	44.4	42.8
ν_3	34.4	35.0	—	—	33.3	—	—	35.6
ν_4	2.1	1.7[e]	—	—	3.7	—	—	3.9

[a] DFPT.
[b] DFT-FD.
[c] DFT-FD-FS.
[d] Substrate not relaxed.
[e] 3.4 meV with anharmonic correction.

it to be attractive by ∼45 meV, while GGA-PBE shows it to be repulsive by ∼75 meV. Experiments [2, 30] suggest that, even below a coverage of one-half monolayer, the interaction of chemisorbed CO molecules is repulsive and estimated to be ∼20 meV at 0.5 ML [2], albeit for chemisorbed CO on Cu(001).

4. Lattice dynamics

In our calculations, we find that the force constants coupling C–O, C–Cu, O–Cu, C–C, and O–O are stiffer in LDA than in GGA. In particular, those between C–C (between neighboring molecules) and C–Cu are, respectively, 20 and 40% larger. The force constants given by both LDA and GGA-PBE reflect that the *in-plane* interactions between neighboring molecules are much smaller than the *out-of-plane* ones, which arise from the perturbation of the C–O bond length. This fact is reflected in the strong (weak) dispersion of the C–O stretch mode (all other modes), as shown later (see figures 2 and 3). Tables 2 and 3 summarize the frequencies obtained for ν_1, ν_2, ν_3, and ν_4 and compare them with those obtained in earlier calculations and experiments. The characterization of the vibrational modes displayed by CO on Cu(001) is presented below. Complete discussion of the modes of the c(2 × 2)-CO/Cu(100) system, including those of the substrate, will be presented elsewhere [31].

Table 3. Frequencies (in meV) at X of the vibrational modes of c(2 × 2)-CO/Cu(001).

	Theory		Experiment
	LDA	PBE	HAS
	This work	This work	Ref [6]
ν_1	254.9	248.2	—
ν_2	54.4	47.0	—
ν_3	34.1	32.7	—
ν_4	−7.4	5.5	5.8

(a) Dispersion of the C–O internal stretch mode (ν_1). LDA and GGA-PBE find that the C–O stretch mode disperses inside the SBZ (see figures 2 and 3) by ∼10 meV at X, as noted from table 3. No contribution from the substrate is observed, as can

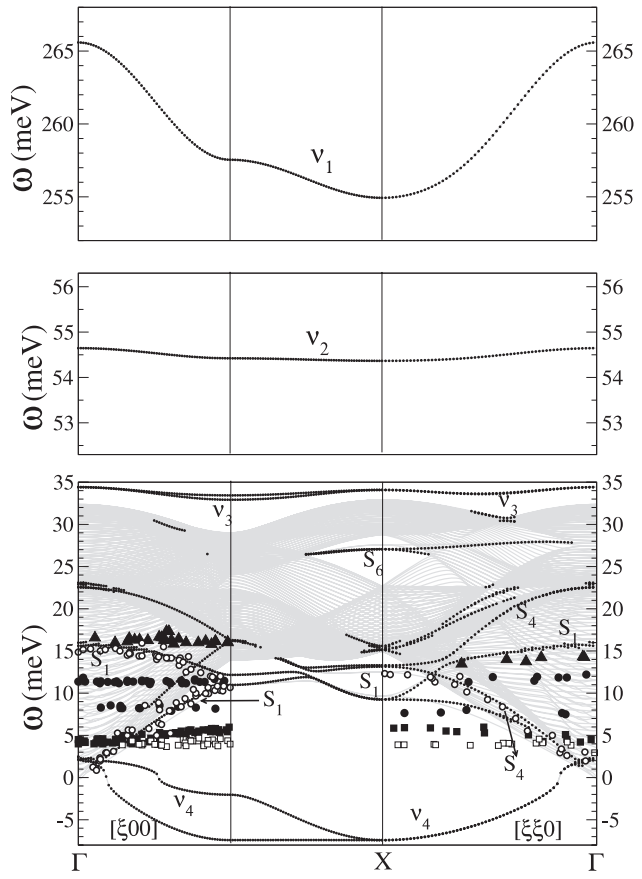

Figure 2. LDA-MB phonon dispersion of c(2 × 2)-CO/Cu(100), modeled by a Cu 50-layer slab. Filled dots denote theoretical surface modes. Experimental data are taken from [6]: filled circles and triangles were associated with multiphonon processes. Open circles correspond to the substrate Rayleigh wave. Squares were associated with the FT mode of CO on the perfect c(2 × 2) structure (filled) and on defects in the adlayer at lower coverage (open).

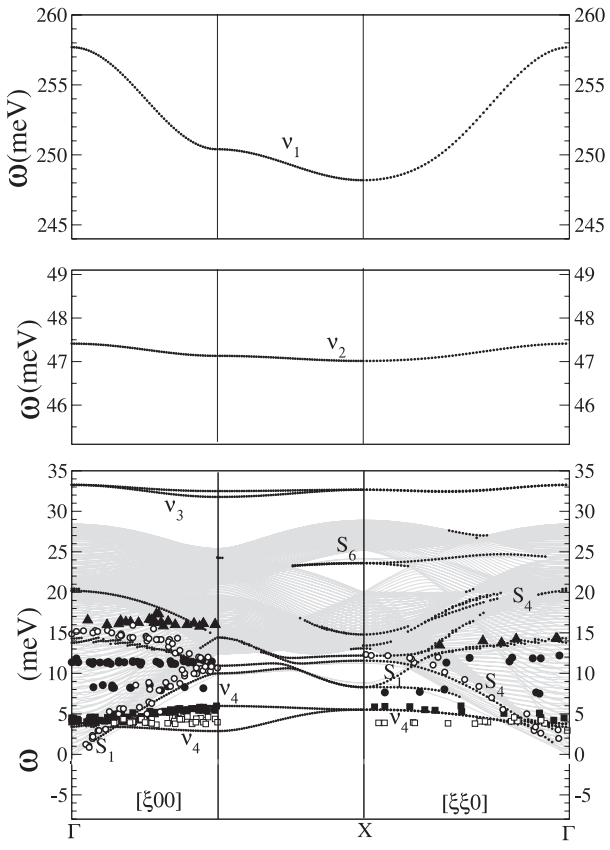

Figure 3. GGA-PBE phonon dispersion of c(2 × 2)-CO/Cu(100), modeled by a Cu 50-layer slab. Filled dots denote theoretical surface modes. Experimental data are taken from [6]: filled circles and triangles were associated with multiphonon processes. Open circles correspond to the substrate Rayleigh wave. Squares were associated with the FT mode of CO on the perfect c(2 × 2) structure (filled) and on defects in the adlayer at lower coverage (open).

be expected from the frequency range in which ν_1 lies. At Γ, small differences are found in the calculated frequencies depending on whether LDA or GGA-PBE is used, whether the FD or the DFPT method is applied, and whether the substrate is frozen (FS) or not. The agreement with experiment is in general reasonable.

(b) Dispersion of the Cu–CO stretch mode (ν_2). As seen in figures 2 and 3, our calculations show that the CO-substrate stretch mode disperses at most by ∼0.4 meV over the sampled region of the SBZ, in both LDA and GGA-PBE. It is found to involve an additional C–O stretching of the C–O bond and to be coupled to an out-of-phase vibration of the Cu atom, which carries ∼33% of the amplitude. LDA, however, predicts $\nu_2 \sim 12$ meV higher than the experimental value, while GGA-PBE finds it to be only ∼5 meV higher, as summarized in table 2.

(c) Frustrated rotation of CO (ν_3). As seen in table 2, the experimental value of ν_3 at Γ is well reproduced by both LDA and GGA. At Γ, LDA and GGA-PBE agree that the contribution of the substrate to the vibrational amplitude reaches only ∼3%, while those of C and O are ∼75 and ∼21%, respectively. Close to X, at which the substrate contribution is maximal, the first and second layers contribute no more than 7%. Figures 2 and 3 show that the FR mode splits along the edge of the SBZ and along the Σ direction, but negligibly along the Δ direction. The maximum splitting reaches ∼0.7 meV at the zone boundary. The branch with lowest energy has shear horizontal (SH) polarization (displacement perpendicular to propagation direction).

(d) Frustrated Translation of CO (ν_4). Significant differences are seen in figures 2 and 3 between LDA and GGA-PBE in relation to the dispersion of the FT mode. It is apparently well described at Γ by LDA [13] because it estimates ν_4 only ∼2 meV below the experimental value. Nonetheless, it is unstable almost everywhere outside Γ. GGA-PBE, on the other hand, is able to reproduce ν_4 in excellent agreement with the experimental assessment, as shown in table 3. GGA-PBE presents no instabilities, and shows remarkable agreement with the HAS data set, indicating stability of the c(2 × 2) overlayer (see figure 3) [6]. The longitudinal (L-) branch (atomic displacement along the propagation direction) and the SH-branch of the FT mode split along Σ and along the edge of the SBZ, but not along Δ, similar to the behavior of the FR mode.

Both LDA and GGA-PBE find that the FT mode couples to the substrate in the vicinity of Γ. Such harmonic resonant coupling is manifested only by a symmetric broadening of the mode. The L-polarized FT branch and the Rayleigh wave hybridize at their crossing point giving rise to two L-polarized FT modes that are split by ∼0.4 meV and show different degrees of contribution from the vertical vibration of the surface. Close to the zone boundaries, the contribution of the substrate to the FT mode is small (∼3%) given that its frequency falls below the bulk band.

5. Summary

First-principles calculations of the structure and lattice dynamics of c(2 × 2)-CO/Cu(100) surfaces have been presented. We find that CO-modes are influenced by molecule–substrate and molecule–molecule interactions. The C–O stretch mode disperses by ∼10 meV along Δ, indicative of CO–CO interactions. Inspection of the displacement vectors in our DFPT calculations confirms that the C–O stretch mode is independent of the dynamics of the substrate. The value of ν_1 is found to be in good agreement with experiment, regardless of the approximation used for the exchange correlation functional.

Nevertheless, the results obtained for ν_2, ν_4, and the structure and vibrational frequencies of the substrate depend on whether LDA or GGA-PBE is used. Our results and those of [12] suggest that this is related to the inability of LDA to describe the Cu–C bond (wrong adsorption site and overestimation of the binding energy [12]). Surprisingly, the value of ν_2 provided by LDA FD-FS calculations is closer to the experimental one than that by LDA-DFPT. The reason is apparently the cancelation of errors, since FD-FS calculations neglect the strong contribution of covered Cu atoms. We find that omission of the dynamics of the substrate lowers ν_2 by ∼8 meV in DFPT calculations. It is thus not surprising that the stiffening due to the overestimation by LDA of the C–Cu bond strength can be counterbalanced by the softening resulting from a frozen substrate. Along the same lines, a much better estimation of ν_2 can be expected from DFPT GGA-PBE calculations since the adsorption site, E_{ch} [12], and d_{Cu-C} are in good agreement with experiment.

In this work, the unsuitability of LDA to describe CO-c(2 × 2) on Cu(001) is evident from the instability of the FT mode almost everywhere inside the SBZ. Such a result signalizes that atop adsorption within LDA renders a minimum that, apart from its local character due to the overestimated hybridization of the $2\pi^*$ orbital with Cu d-states, is not able to bind the molecule under the geometric distortions involved in the FT mode. GGA-PBE, in contrast, is able to reproduce the dispersion of the FT mode as measured by HAS [6], affirming that GGA-PBE, which apparently introduces a correction to the interaction of metal d-states with the 5σ and the $2\pi^*$ orbitals, properly describes the Cu–CO interaction. Most importantly, the close agreement between our GGA-PBE calculations and HAS measurements indicates that the harmonic approximation is apt to describe the Cu–CO bond and shows that the FT is a normal mode of the system, contrary to the conclusion drawn from LDA finite-differences approach [13].

Examination of the real-space force constant matrices indicates that lateral interactions among CO molecules exist as well. They are at least 10 times smaller than those due to the perturbation to the C–O bond length, but enough to make the FT and the FR (to a lesser degree) modes to disperse and split their SH- and L-branches, which otherwise would be degenerate. Splitting of the branches of the FT mode along Σ also suggest that the lateral interaction between molecules is repulsive, since the frequency of the SH-branch—which displacement pattern does not drives the CO molecules one against the other—is 3 meV lower than that of the L-branch. Clearly, the SH-branch cannot explain the low branch observed experimentally, which is rather attributed to defects in the overlayer. [6] Finally, the frequency range of the FT mode allows for coupling to the substrate over a significant region around Γ. Such harmonic resonant coupling is manifested only through the broadening of the spectral line of the FT mode, but its frequency (the center of the distribution) is found to be independent of the dynamics of the substrate.

We remind the reader that the conclusions presented in this work correspond solely to the Hedin–Lundqvist (LDA) and PBE (GGA) exchange–correlation functionals. Nevertheless, LDA total energy calculations using Perdew–Zunger parameterization [32]—not presented in the present work for the sake of clarity—find consistently that the fourfold hollow site is preferred [12] over the top one. Mapping of the potential energy surface for displacements of the molecule along the [110] direction shows in addition that the atop local minimum obtained is extremely shallow, while the binding energy at the intermediate sites, such as *hollow-top* and *bridge-top* lie well below that corresponding to atop adsorption [12]. Moreover, instabilities of the FT mode were also found by using the Perdew–Zunger expression [32] for the LDA exchange–correlation functional.

Acknowledgments

This work was supported in part by grant CHE-0741423 from NSF-USA. Computations were performed at the Institut für Festkörperphysik, Forschungszentrum Karlsruhe, Germany. Marisol Alcántara Ortigoza is thankful to Forschungszentrum Karlsruhe for financial support during her stays in Karlsruhe.

References

[1] Gajdos M and Hafner J 2005 *Surf. Sci* **590** 117
[2] Tracy J C 1972 *J. Chem. Phys.* **56** 2748
[3] Lewis S P and Rappe A M 1996 *Phys. Rev. Lett.* **77** 5241
[4] Heid R and Bohnen K P 2003 *Phys. Rep.* **387** 151
[5] Hirschmugl C, Williams G, Hoffmann F and Chabal Y 1990 *Phys. Rev. Lett.* **65** 480
[6] Ellis J, Toennies J P and Witte G 1995 *J. Chem. Phys.* **102** 5059
[7] Fouquet P, Olsen R A and Baerends E J 2003 *J. Chem. Phys.* **119** 509
[8] Andersson S and Pendry J B 1979 *Phys. Rev. Lett.* **43** 363

[9] McConville C F, Woodruff D P, Prince K C, Paolucci G, Chab V, Surman M and Bradshaw A M 1986 *Surf. Sci.* **166** 221
[10] Stöhr J, Gland J, Eberhardt W, Outka D, Madix R, Sette F, Koestner R and Doebler U 1983 *Phys. Rev. Lett.* **51** 2414
[11] Graham A P, Hofmann F, Toennies J P, Williams G P, Hirschmugl C J and Ellis J 1998 *J. Chem. Phys.* **108** 7825
[12] Favot F, Corso A D and Baldereschi A 2001 *J. Chem. Phys.* **114** 483
[13] Lewis S P and Rappe A M 1999 *J. Chem. Phys.* **110** 4619
[14] Kohanoff J and Gidopoulos N I 2003 *Handbook of Molecular Physics and Quantum Chemistry* 1st edn (Chichester: Wiley)
[15] Ciofini I, Adamo C and Chermette H 2005 *Chem. Phys.* **309** 67
[16] Kresse G, Gil A and Sautet P 2003 *Phys. Rev.* B **68** 073401
[17] Hu Q M, Reuter K and Scheffler M 2007 *Phys. Rev. Lett.* **98** 176103
[18] Neef M and Doll K 2006 *Surf. Sci.* **600** 1085
[19] Mason S E, Grinberg I and Rappe A M 2004 *Phys. Rev.* B **69** 161401(R)
[20] Gil A, Clotet A, Ricart J M, Kresse G, García-Hernández M, Rösch N and Sautet P 2003 *Surf. Sci.* **530** 71
[21] Louie S G, Ho K M and Cohen M L 1979 *Phys. Rev.* B **19** 1774
[22] Hedin L and Lundqvist B I 1971 *J. Phys. C: Solid State Phys.* **4** 2064
[23] Perdew J P, Burke K and Ernzerhof M 1996 *Phys. Rev. Lett.* **77** 3865
[24] Gillan M J 1989 *J. Phys.: Condens. Matter* **1** 689
[25] Payne M C, Teter M P, Allan D C, Arias T A and Joannopoulos J D 1992 *Rev. Mod. Phys.* **64** 1045
[26] Press W H, Teukolsky S A, Vetterling W T and Flannery B P 1992 *Numerical Recipes in Fortran The Art of Scientific Computing* 2nd edn (Cambridge: Cambridge University Press)
[27] Baroni S, Giannozzi P and Testa A 1987 *Phys. Rev. Lett.* **58** 1861
[28] Heid R and Bohnen K P 1999 *Phys. Rev.* B **60** R3709
[29] Gianozzi P, Gironcoli S, Pavone P and Baroni S 1991 *Phys. Rev.* B **43** 7231
[30] Peterson L D and Kevan S D 1991 *J. Chem. Phys.* **94** 2281
[31] Alcántara Ortigoza M, Heid R, Bohnen K P and Rahman T S 2008 unpublished
[32] Zunger J P and Zunger A 1981 *Phys. Rev.* B **23** 5048
[33] DeFrees D J, Levi B A, Hehre W J, Pollack S K, Binkley J S and Pople J A 1979 *J. Am. Chem. Soc.* **101** 4085
[34] Philipsen P H T, te Velde G and Baerends E J 1994 *Chem. Phys. Lett.* **226** 583